

Table II. Kinetic Data for Electrocatalytic Reductions with Vitamin B₁₂

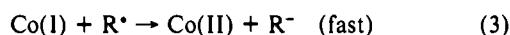
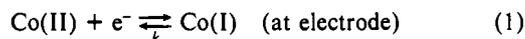
| [B ₁₂], ^a mM | scan rate, mV s ⁻¹ | E _p ^b V vs SCE | i _c /2γi _p | 10 ⁻⁵ k _{obs} , M ⁻¹ s ⁻¹ |
|--|----------------------------------|---|----------------------------------|---|
| Chloroacetic Acid | | | | |
| 1.03 | 100 | 0.811 | 0.546 | 0.063 |
| | 80 | 0.811 | 0.640 | 0.075 |
| | 50 | 0.818 | 0.628 | 0.043 |
| | 30 | 0.814 | 0.780 | 0.040 |
| 1.23 | 100 | 0.814 | 0.522 | 0.060 |
| | 80 | 0.811 | 0.655 | 0.065 |
| | 50 | 0.806 | 0.811 | 0.058 |
| Trichloroacetic Acid | | | | |
| 1.02 | 200 | 0.727 | 1.86 | 2.5 |
| | 100 | 0.724 | 1.83 | 1.1 |
| | 80 | 0.727 | 2.10 | 1.4 |
| | 50 | 0.718 | 2.25 | 1.1 |
| Bromoacetic Acid | | | | |
| 1.03 | 200 | 0.725 | 1.62 | 1.7 |
| | 100 | 0.716 | 1.70 | 0.91 |
| | 80 | 0.729 | 1.57 | 0.53 |
| | 50 | 0.723 | 1.61 | 0.35 |
| 1.22 | 200 | 0.737 | 1.52 | 1.1 |
| | 100 | 0.730 | 1.73 | 0.82 |
| | 80 | 0.739 | 1.79 | 0.81 |
| 0.89 ± 0.44 (mean) | | | | |

^a Acetonitrile/water (1:1), pH 3 phosphate buffer; haloacetic acid concentrations were 10[B₁₂]. ^b All entries are the average of three or more CV scans.

acid yielded about half of its total Cl⁻ in 5 h, again with about 2 faradays/mol of Cl⁻ passed through the cell. Electrolyses of the trihalo acids showed that more than one halide per acid molecule was removed. Less than 2 faradays/mol of Br⁻ was found for tribromoacetic acid, where unknown competing reactions may occur.¹¹ These experiments confirmed that the predominant reaction of α-haloacetic acids with cob(I)alamin is two-electron cleavage of carbon-halogen bonds.

After trichloroacetic acid was added to a pH 3 solution containing a stoichiometric amount of cob(I)alamin, titration indicated that the trichloroacetic acid released 94% of its Cl⁻ (Table I). The UV-vis spectrum of the vitamin B₁₂ before electrolysis was nearly identical with that after electrolysis and addition of halo acid. These results suggest that dehalogenation of halo acids by cob(I)alamin is spontaneous and does not involve electroreduction of a stable organocobalt intermediate.

Kinetics. Rate constants were estimated by comparing catalytic efficiencies obtained by CV (see Experimental Section) to computer simulations based on the scheme



The rate-determining step is assumed to be the reaction of cob(I)alamin with the halo acid (eq 2), as in other reactions of this type.¹² Equation 3 is kinetically invisible because of its rapid rate. It is used in the simulated reduction as the source of the second electron, a process for which alternatives exist.² R⁻ presumably undergoes protonation in the weakly acidic reaction medium.

Observed rate constants were estimated for three halo acids.¹¹ As expected, the more easily reduced trichloroacetic acid gave a rate constant about 25 times larger than that of chloroacetic acid (Table II). This suggests that the catalytic reduction, like direct electrolysis,^{9,10} proceeds in a stepwise fashion. The rate

constant for bromoacetic acid was similar to that of trichloroacetic acid but 15-fold larger than that of chloroacetic acid, consistent with the greater ease of reduction of C-Br bonds.¹²

Conclusions. Reductive dehalogenation of the α-haloacetic acids to acetic acid can be achieved by cob(I)alamin. To our knowledge, this is a new example of electrocatalytic reduction by vitamin B₁₂, in which a reduced organic product is formed directly at the formal potential of Co(II)/Co(I). Dehalogenation of halo acids by cob(I)alamin is spontaneous. If an organocobalt intermediate exists, it must be made reductively unstable by the carboxylic acid group. These reactions are similar to dehalogenation of vicinal dihalides to alkenes by cob(I)alamin.² Characteristic large catalytic currents for these reactions are in contrast to the behavior of monohaloalkanes with vitamin B₁₂, for which catalytic currents are not observed at the Co(II)/Co(I) potential, and more negative potentials are needed to decompose the stable alkylcob(III)alamins formed.^{5,13}

Comparison of direct reduction potentials of the halo acids⁸ with potentials of the B₁₂-mediated reductions (Table II) shows that overpotentials for dehalogenation are decreased by 0.75–1.4 V by electrocatalysis. These large decreases in overpotential and the high catalytic rate constants suggest an inner-sphere mechanism. The reduction of vicinal dihalides by cob(I)alamin was inferred to be inner sphere from comparative kinetic studies with known outer-sphere reductants.^{4,14}

Acknowledgment. This work was supported by U.S. PHS Grant ES03154 awarded by the National Institute of Environmental Health Sciences and partly by the Environmental Research Institute, College of Engineering, University of Connecticut. We thank Rosanne Slingsby of Dionex Corp. for initiating interest in haloacetic acids and for the gift of the α-haloacetic acids.

- (12) (a) Perichon, J. In *Encyclopedia of Electrochemistry of the Elements*; Bard, A. J., Lund, H., Eds.; Marcel Dekker: New York, 1978; Vol. XI, pp 72–162. (b) The small variation of k_{obs} with scan rate for trichloro and bromo acids suggests that the complete reaction mechanism may be more complex than the simple catalytic scheme used to treat the kinetic data.
- (13) Lexa, D.; Saveant, J. M.; Soufflet, J. P. *J. Electroanal. Chem. Interfacial Electrochem.* **1979**, *100*, 159.
- (14) Lexa, D.; Saveant, J. M.; Su, K. B.; Wang, D. L. *J. Am. Chem. Soc.* **1987**, *109*, 6464.

Contribution from the Department of Chemistry,
University of Florida, Gainesville, Florida 32611

Preparation, Solution Dynamics, and X-ray Crystal Structure of the Anilide-Bridged Diruthenium Complex [(η⁶-C₆Me₆)₂Ru₂(μ-NHPh)₃][BF₄]

Gaines C. Martin, Gus J. Palenik, and James M. Boncella*

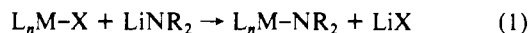
Received June 12, 1989

There has been increasing interest in the potential use of transition-metal amide complexes to facilitate the formation of carbon-nitrogen bonds.¹ One class of compounds that is of particular interest in this regard is late-transition-metal amide complexes. A problem that limits the use of these compounds is a lack of general synthetic routes to such materials. Consequently, there are relatively few reported examples of late-transition-metal amides.² Typically, these compounds have been

(11) Although catalytic current was also observed for tribromoacetic acid with vitamin B₁₂, subsequent scans showed the appearance of unexplained peaks. These new peaks suggested possible side reactions. Thus, rate constants were not estimated for this compound.

(1) Bryndza, H. E.; Tam, W. *Chem. Rev.* **1988**, *88*, 1163.
(2) (a) Cowan, R. L.; Trogler, W. C. *J. Am. Chem. Soc.* **1989**, *111*, 4750.
(b) Bryndza, H. E.; Fultz, W. C.; Tam, W. *Organometallics* **1985**, *4*, 939. (c) Cowan, R. L.; Trogler, W. C. *Organometallics* **1987**, *6*, 2451.
(d) Bryndza, H. E.; Fong, L. K.; Paciello, R. A.; Tam, W.; Bercaw, J. E. *J. Am. Chem. Soc.* **1987**, *109*, 1444. (e) Hope, H.; Olmstead, M. M.; Murray, B. O.; Power, P. P. *J. Am. Chem. Soc.* **1985**, *107*, 712. (f) Olmstead, M. M.; Power, P. P.; Sigel, G. *Inorg. Chem.* **1986**, *25*, 1027.
(g) Bartlett, R. A.; Power, P. P. *J. Am. Chem. Soc.* **1987**, *109*, 7563.
(h) Koch, S.; Miller, M. *J. Am. Chem. Soc.* **1982**, *104*, 5255.

synthesized by metathetical exchange of halide (or other leaving group) with a group I amide compound as shown in eq 1.¹



Although this technique is useful under some circumstances, an alternative to this synthetic method would be useful since reduction of the transition-metal fragment and nucleophilic attack on coordinated ligand are competing side reactions that limit the utility of the reaction in eq 1.

One alternative that may be effective in general is the deprotonation of a primary or secondary amine that is coordinated to a metal cation, as shown in eq 2. This method takes advantage



of the fact that an amine becomes much more acidic when it coordinates to a Lewis acid. Recently, this technique has proven successful in the synthesis of some amide complexes of the later transition metals.³ Since our initial attempts at the synthesis of amide complexes via the reaction of $(\eta^6-C_6Me_6)Ru(PMe_3)_2X_2$ ($X = Cl, I$) with a variety of $LiNR_2$ reagents (eq 1) produced intractable mixtures of products, we chose to examine the use of eq 2 for the synthesis of these compounds. Reported here are the results of these studies starting with the compound $[(\eta^6-C_6Me_6)Ru(PMe_3)(Cl)(NH_2Ph)][BF_4]$ (**1**).

Experimental Section

All procedures were carried out under an atmosphere of argon. The compounds $[(\eta^6-C_6Me_6)RuCl_2]_2$ and $(\eta^6-C_6Me_6)Ru(PMe_3)Cl_2$ were prepared by using literature procedures.^{4,5} Solvents and reagents were dried and deoxygenated by using standard methods prior to use, and $LiN(SiMe_3)_2$ was used as a 1 M solution in hexanes (Aldrich). NMR spectra were obtained at either 100 MHz on a JEOL FX 100 spectrometer or at 300 MHz on a Varian VXR 300 spectrometer. Chemical shifts were referenced to residual proton signals in the solvent and are reported relative to TMS. Elemental analyses were performed by Atlantic Microlabs, Inc., or the analytical services of this department.

Preparation of $[(\eta^6-C_6Me_6)Ru(PMe_3)(Cl)(NH_2Ph)][BF_4]$ (1**).** To a solution of $(\eta^6-C_6Me_6)Ru(PMe_3)Cl_2$ (0.147 g, 0.358 mmol) in 20 mL of CH_2Cl_2 was added 20 mL of a stirred suspension of $AgBF_4$ (0.070 g, 0.350 mmol) and aniline (0.33 mL, 0.350 mmol) in CH_2Cl_2 . The reaction mixture rapidly changed color from red to yellow-brown, accompanied by the formation of large amounts of white precipitate. The mixture was stirred for 3 h and allowed to settle. The supernatant was then filtered off and the solvent evaporated, leaving a yellow-brown residue. Thorough washing with pentane and diethyl ether and drying under reduced pressure gave the crude product as a yellow solid (0.155 g, 0.279 mmol). Yield: 78%. Recrystallization from dichloromethane/diethyl ether gave yellow crystals. Anal. Calcd for $C_{21}H_{34}BClF_4NPRu$: C, 45.46; H, 6.18; N, 2.52. Found: C, 45.47; H, 6.22; N, 2.50. ¹H NMR: δ 7.68 (2 H, d of m, ortho C-H), 7.32 (2 H, t of m, meta C-H), 7.19 (1 H, t of m, para C-H), 5.95 (1 H, d, ²J_{H-H} = 9.4 Hz, N-H), 4.03 (1 H, d, ²J_{H-H} = 9.40 Hz, N-H), 1.85 (18 H, s, Me_6C_6), 1.58 (9 H, d, ³J_{P-H} = 10.4 Hz, pMe_3). ¹³C NMR: δ 144.1 (Ar), 129.2 (Ar), 126.1 (Ar), 122.5 (Ar), 97.37 (C_6Me_6), 15.50 (C_6Me_6), 14.22 (d, $J_{P-C} = 28$ Hz, pMe_3). ³¹P NMR: δ 41.54.

Preparation of $[(\eta^6-C_6Me_6)_2Ru(\mu-NHPh)_3][BF_4]$ (2**).** A solution of **1** (0.203 g, 0.366 mmol) in 10 mL of THF was cooled to -10 °C. To this solution was added 0.37 mL of a 1.0 M solution of $LiN(SiMe_3)_2$ in hexanes. The reaction mixture immediately darkened. The ice bath was removed, and the solution was allowed to warm to room temperature. A bright yellow microcrystalline precipitate formed as the solution was allowed to warm. The reaction mixture was stirred for ca. 12 h, and the precipitate was collected and dried under reduced pressure to give 0.053 g (0.06 mmol) of crude product. Yield: 30% based on ruthenium. The compound can be recrystallized by cooling a concentrated CH_2Cl_2 /pentane solution (ca. 1:1 v/v) to give analytically pure crystals of **2**. Crystals suitable for X-ray diffraction studies were obtained by layering a CH_2Cl_2 solution of **2** with pentane. The presence of CH_2Cl_2 in the lattice of crystals grown in this manner was confirmed by ¹H NMR spectroscopy. Anal. Calcd for $C_{42}H_{34}BF_4N_3Ru_2$: C, 56.69; H, 6.12; N, 4.72. Found:

Table I. Crystal Data for $[(\eta^6-C_6Me_6)_2Ru_2(\mu-NHPh)_3][BF_4]$ (**3**)

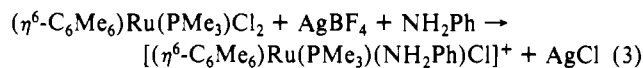
| | | | |
|---------|-------------------------------|----------------|------------------------|
| formula | $C_{42}H_{34}N_3BCl_2F_4Ru_2$ | space group | Cc (No. 9) |
| fw | 974.79 | T | 25 °C |
| a | 10.7118 (12) Å | λ | 0.71 Å |
| b | 20.8580 (12) Å | ρ_{calcd} | 1.507 cm ⁻³ |
| c | 19.2407 (12) Å | μ | 8.6 cm ⁻¹ |
| β | 91.770 (14)° | R | 0.045 |
| V | 4296.8 Å ³ | R_w | 0.058 |
| Z | 4 | | |

C, 56.55; H, 6.07; N, 4.63. ¹H NMR ($CDCl_3$): δ 7.45 (3 H, t of d, ³J_{H-H} = 7.75 Hz, meta or para H), 7.35 (3 H, d of m, ³J_{H-H} = 8.35 Hz, ortho H), 7.30 (3 H, t of m, ³J_{H-H} = 7.45 Hz meta or para H), 7.06 (3 H, t of m, ³J_{H-H} = 7.70 Hz, meta or para H), 6.84 (3 H, d of m, ³J_{H-H} = 8.06 Hz, ortho H), 2.39 (3 H, s, N-H), 1.36 (36 H, s, C_6Me_6). ¹³C NMR ($CDCl_3$): δ 156.5 (ipso C), 130.7 (meta or ortho C), 128.7 (meta or ortho C), 124.7 (meta or ortho C), 122.9 (meta or ortho C), 117.7 (para C), 90.5 (C_6Me_6), 14.6 (C_6Me_6).

X-ray Data Collection, Structure Solution, and Refinement of **2.** A crystal was sealed in a thin-walled X-ray capillary to minimize decomposition and loss of solvent. A Nicolet R3m diffractometer was used for all the measurements. The pertinent data are summarized in Table I. The SHELXTL system on a Model 30 Desktop Eclipse and local programs were used in the analysis. The systematic absences were consistent with the space groups Cc and $C2/c$, but intensity statistics and the Patterson function suggested the acentric space group Cc . The Ru positions were determined from the Patterson function and the light atoms from successive Fourier syntheses. Refinement of the structure was by full-matrix least squares with isotropic thermal parameters and then with only the two Ru atoms anisotropic. Final refinement was by blocked least squares with all atoms anisotropic. The BF_4^- and H_2CCl_2 species had relatively large thermal motion and the four F atoms and two Cl atoms were included as half-atoms. The final difference Fourier synthesis showed some residual electron density in the vicinity of both groups. The addition of other half-atoms for these two groups would be largely cosmetic. The final positional parameters are given in Table II. Selected bond distances are given in Table III. Tables of anisotropic thermal parameters, bond distances and angles, and structure factor amplitudes are available—see paragraph at end of the paper regarding supplementary material.

Results and Discussion

Complex **1** was synthesized by abstraction of chloride from the compound $(\eta^6-C_6Me_6)Ru(PMe_3)Cl_2$ using $AgBF_4$ in the presence of 1 equiv of aniline, as shown in eq 3. Compound **1** can be isolated as air-stable yellow crystals by layering a CH_2Cl_2 solution with pentane.



When **1** is treated with 1 equiv of $LiN(SiMe_3)_2$ at -10 °C, the solution darkens immediately, and as the reaction mixture warms to room temperature, a yellow microcrystalline precipitate of **2** begins to form. The precipitation of **2** is complete in ca. 12 h. The ³¹P NMR spectrum of this material indicates that there is no pMe_3 present in the sample. Furthermore, examination of the ¹H NMR spectrum reveals that there are hexamethylbenzene rings and anilide groups in a 2:3 ratio. Compound **2** was ultimately characterized by a single-crystal X-ray diffraction study. The material that precipitates from the reaction mixture is pure as judged by ¹H NMR spectroscopy; however, it may be recrystallized from CH_2Cl_2 and pentane to obtain an analytically pure sample. The THF-soluble portion of the reaction mixture contains small amounts of **2** as well as $(\eta^6-C_6Me_6)Ru(PMe_3)Cl_2$ (**3**) and $[(\eta^6-C_6Me_6)Ru(PMe_3)_2Cl][BF_4]$ (**4**) as the only hexamethylbenzene-containing products observable via ¹H NMR spectroscopy. We have not studied the mechanism of formation of these products due to the complexity of the reaction. The observation of the formation of **3** and **4** in quantities comparable to that of **2** suggests that a disproportionation reaction is occurring which ultimately limits the overall yield of **2** in this reaction.

X-ray Diffraction Study

Single crystals of compound **2** were obtained by solvent diffusion of pentane into a CH_2Cl_2 solution of **2**. The single-crystal X-ray diffraction study of **2** reveals that the compound consists of cations of the stoichiometry $[(\eta^6-C_6Me_6)_2Ru]_2(\mu-NHPh)_3^+$ and BF_4^-

- (3) (a) Klein, D. P.; Hayes, J. C.; Bergman, R. G. *J. Am. Chem. Soc.* **1988**, *110*, 3704. (b) Park, S.; Roundhill, D. M.; Rheingold, A. L. *Inorg. Chem.* **1987**, *26*, 3972.
 (4) Bennett, M. A.; Huang, T.-N.; Matheson, T. W.; Smith, A. K. *Inorg. Synth.* **1982**, *21*, 74.
 (5) Werner, H.; Kletzen, H. *J. Organomet. Chem.* **1982**, *228*, 289.

Table II. Final Atomic Coordinates ($\times 10^4$) for $[(\eta^6\text{-C}_6\text{Me}_6)_2\text{Ru}_2(\mu\text{-NHPPh})_3][\text{BF}_4]\cdot\text{CH}_2\text{Cl}_2$

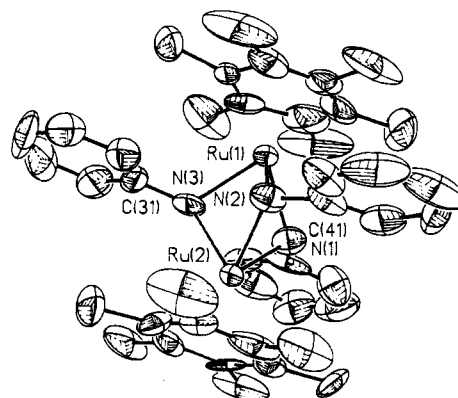
| atom | x/a | y/b | z/c |
|-------|-------------------|------------|-------------------|
| Ru(1) | 5000 ^a | 3388.6 (4) | 5000 ^a |
| Ru(2) | 7734 (1) | 36585 (4) | 54099 (6) |
| N(1) | 6756 (10) | 3184 (6) | 4561 (6) |
| N(2) | 6239 (11) | 3161 (6) | 5873 (6) |
| N(3) | 3111 (10) | 4226 (6) | 5200 (7) |
| C(11) | 3158 (14) | 3279 (9) | 5487 (8) |
| C(12) | 3162 (11) | 3849 (6) | 5068 (9) |
| C(13) | 3500 (12) | 3789 (8) | 4345 (8) |
| C(14) | 3795 (18) | 3104 (13) | 4084 (11) |
| C(15) | 3784 (16) | 2630 (9) | 4530 (11) |
| C(16) | 3481 (14) | 2691 (8) | 5183 (10) |
| C(21) | 9610 (13) | 3256 (7) | 5291 (9) |
| C(22) | 9327 (15) | 3235 (9) | 6014 (10) |
| C(23) | 8926 (11) | 3762 (7) | 6338 (6) |
| C(24) | 8891 (13) | 4367 (8) | 6001 (9) |
| C(25) | 9139 (13) | 4408 (7) | 5277 (9) |
| C(26) | 9560 (10) | 3821 (8) | 4938 (7) |
| C(31) | 5699 (13) | 4729 (8) | 5675 (9) |
| C(32) | 5596 (18) | 5309 (10) | 5354 (12) |
| C(33) | 5220 (24) | 5829 (9) | 5737 (13) |
| C(34) | 4940 (21) | 5776 (9) | 6412 (13) |
| C(35) | 5055 (19) | 5185 (12) | 6770 (11) |
| C(36) | 5449 (16) | 4645 (8) | 6350 (11) |
| C(41) | 6375 (13) | 2469 (7) | 6098 (9) |
| C(42) | 6122 (16) | 2394 (9) | 6772 (10) |
| C(43) | 6155 (18) | 1790 (14) | 7069 (11) |
| C(44) | 6465 (21) | 1260 (12) | 6719 (13) |
| C(45) | 6702 (21) | 1340 (10) | 6041 (16) |
| C(46) | 6677 (15) | 1960 (11) | 5722 (9) |
| C(51) | 7036 (14) | 3343 (9) | 3847 (7) |
| C(52) | 6897 (16) | 3946 (10) | 3530 (10) |
| C(53) | 7230 (20) | 4009 (12) | 2822 (11) |
| C(54) | 7760 (22) | 3552 (11) | 2495 (11) |
| C(55) | 7833 (23) | 2959 (13) | 2792 (13) |
| C(56) | 7489 (20) | 2861 (10) | 3475 (10) |
| C(61) | 2831 (21) | 3384 (16) | 6242 (10) |
| C(62) | 2612 (20) | 4460 (10) | 5356 (14) |
| C(63) | 3487 (21) | 4413 (13) | 3902 (14) |
| C(64) | 4077 (27) | 3074 (12) | 3281 (11) |
| C(65) | 4210 (23) | 1971 (12) | 4183 (17) |
| C(66) | 3371 (20) | 2055 (13) | 5593 (18) |
| C(71) | 9951 (18) | 2603 (10) | 4924 (17) |
| C(72) | 9445 (22) | 2637 (11) | 6466 (15) |
| C(73) | 8562 (20) | 3707 (13) | 7123 (19) |
| C(74) | 8598 (22) | 4988 (11) | 6344 (16) |
| C(75) | 9107 (20) | 5022 (10) | 4858 (15) |
| C(76) | 9912 (19) | 3827 (14) | 4166 (11) |
| C(08) | 2196 (39) | 4107 (17) | 8044 (22) |
| Cl(1) | 1705 (11) | 4653 (5) | 7521 (6) |
| Cl(2) | 1700 (15) | 4027 (6) | 8896 (8) |
| B(1) | 6119 (67) | 3950 (29) | 8487 (23) |
| F(1) | 5559 (38) | 4419 (13) | 8510 (15) |
| F(2) | 6470 (36) | 3343 (24) | 8514 (25) |
| F(3) | 5269 (32) | 3708 (14) | 7759 (13) |
| F(4) | 4903 (36) | 3650 (15) | 8917 (13) |

^a Value fixed because of space group restrictions.

Table III. Selected Bond Lengths (Å) and Angles (deg) for $[(\eta^6\text{-C}_6\text{Me}_6)_2\text{Ru}_2(\mu\text{-NHPPh})_3][\text{BF}_4]\cdot\text{CH}_2\text{Cl}_2$

| Bond Distances | | |
|------------------|-------------|---------------------------------------|
| Ru(1)–Ru(2) | 3.062 (1) | Ru(2)–N(1) 2.154 (11) |
| Ru(1)–N(1) | 2.128 (11) | Ru(2)–N(2) 2.127 (12) |
| ru(1)–N(2) | 2.160 (12) | Ru(2)–N(3) 2.131 (11) |
| Ru(1)–N(3) | 2.141 (12) | Ru2-C _{ring} (av) 2.206 (18) |
| Bond Angles | | |
| Ru(1)–N(1)–Ru(2) | 91.27 (45) | Ru(1)–N(2)–C(41) 118.95 (89) |
| Ru(1)–N(2)–Ru(2) | 91.15 (47) | Ru(2)–N(2)–C(41) 121.19 (85) |
| Ru(1)–N(3)–Ru(2) | 91.54 (47) | Ru(1)–N(3)–C(31) 121.22 (84) |
| Ru(1)–N(1)–C(51) | 122.73 (92) | Ru(1)–N(3)–C(31) 122.55 (92) |
| Ru(2)–N(1)–C(51) | 120.13 (96) | |

counterions. When crystallized in this fashion, one molecule of CH_2Cl_2 cocrystallizes with each cation. The presence of the CH_2Cl_2 in the crystals used for the X-ray study was confirmed

**Figure 1.** ORTEP drawing of $[(\eta^6\text{-C}_6\text{Me}_6)_2\text{Ru}_2(\mu\text{-NHPPh})_3]^+$. Thermal ellipsoids are at the 50% probability level.

by ^1H NMR spectroscopy. The coordination sphere around each Ru atom consists of an $\eta^6\text{-C}_6\text{Me}_6$ ring and three anilide nitrogen atoms that bridge the two metal centers. An ORTEP drawing of the compound is shown in Figure 1. Table III contains a summary of bond lengths and angles in the cation.

The Ru–N distances are equal to within experimental error and reveal that the anilide groups bridge the two ruthenium centers symmetrically. The Ru–Ru distance is 3.062 Å and is too long for a Ru–Ru bond. The Ru–N–Ru angles average 91° , while the Ru–N–C angles vary between 118 and 122° . Thus, the geometry about N is that of a distorted tetrahedron. The overall geometry is analogous to the well-known class of molecules $\text{L}_3\text{Ru}(\mu_2\text{-X})_3\text{RuL}_3$, which can be described as cofacial bioctahedra.⁶ In **2** the hexamethylbenzene ligands replace the L_3 group and the anilides function as X. The pair of hydroxo-bridged dimers $[(\eta^6\text{-1,3,5-R}_3\text{C}_6\text{H}_3)_2\text{Ru}_2(\mu\text{-OH})_3]^+$ (R = CH_3 (**5**), H (**6**)) are structurally similar to **2** with Ru–O–Ru angles of 90 and 91° , respectively.^{7,8} However, the Ru–Ru distances in **5** and **6** are shorter (2.981 and 2.987 Å) than in **2** and the Ru–O bond length (2.07–2.09 Å) is shorter than the average Ru–N bond length of 2.14 Å. These structural differences most probably arise from the extremely short nonbonded interactions between the C_6Me_6 groups and the anilide groups in **2**.

Perhaps the most noteworthy facet of the structure is the extreme steric crowding that occurs within the molecule. There are short contacts between three of the methyl groups on each C_6Me_6 ring and the three ipso carbon atoms of the anilide groups. These contacts vary between 3.26 and 3.40 Å. The C_6Me_6 rings are staggered with respect to the anilide nitrogen atoms, and the contacts between the ring carbons and the anilide nitrogen that they straddle vary between 3.25 and 3.40 Å. This extreme crowding causes all three anilide phenyl rings and the two hexamethylbenzene rings to pack in an essentially coplanar fashion. The distance between the two C_6Me_6 rings is 6.45 Å, while the distance between the C_6Me_6 planes and the plane defined by the three $\text{C}_6\text{H}_5\text{N}$ groups is 3.22 Å. Clearly, the C_6Me_6 rings and anilide groups are essentially closest packed and account for the rather long Ru–Ru distance relative to those found in the hydroxo-bridged cations.

NMR Studies

In the solid state, there is a noncrystallographic 3-fold symmetry axis that passes through the two Ru atoms and equates all three anilide groups. If this structure exists in solution, then the three anilide groups will be equivalent, as observed via ^1H NMR spectroscopy. If rotation about the C–N bond is rapid on the ^1H NMR time scale, then three signals will be observed, one each for the ortho, meta, and para phenyl protons, respectively.

- (6) Seddon, E. A.; Seddon, K. R. *The Chemistry of Ruthenium*; Elsevier: New York, 1984.
 (7) Gould, R. O.; Jones, C. L.; Stephenson, T. A.; Tocher, D. A. *J. Organomet. Chem.* **1984**, *264*, 365.
 (8) King, T. O.; McNeese, T. J.; Rheingold, A. L. *Inorg. Chem.* **1988**, *27*, 2554.

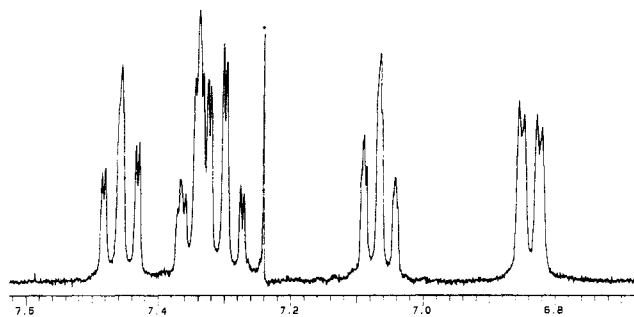


Figure 2. 300-MHz ^1H NMR spectrum (CDCl_3) of the phenyl region of **2**. The asterisk denotes residual CHCl_3 .

temperature, as shown in Figure 2. The coupling pattern and intensity ratios are consistent with the crystal structure of the compound if rotation about the N-phenyl bond is slow on the NMR time scale. The $^{13}\text{C}\{^1\text{H}\}$ NMR spectrum (25 MHz) up to 100 °C reveals six aromatic resonances and is also consistent with hindered rotation about the N-C bond. Variable-temperature ^{13}C NMR studies in $\text{DMSO}-d_6$ show that the two ortho and two meta aromatic carbon resonances broaden and disappear into the base line at 150 °C. Coalescence of these peaks is not observed even at 175 °C. Use of the two-site-exchange approximation⁹ allows estimation of a lower limit for the ΔG^\ddagger for N-C bond rotation of ca. 21 kcal mol⁻¹.

This large energy of activation for rotation about an N-C single bond is comparable to the barriers observed for rotation about the N-C bonds of organic amides.¹⁰ However, the crystallographic study revealed a nearly tetrahedral environment around each N in the molecule, suggesting that the hindered rotation is not caused by π bonding between the nitrogen and the phenyl ring. The restricted phenyl ring rotation must therefore arise from the extremely crowded environment of the molecule.

The observation that compound **2** is isolable and stable to 175 °C in DMSO indicates that the Ru-N bond in this amide complex is rather robust. The use of the method of deprotonation of coordinated amines in the synthesis of metal amides is a viable possibility. In this case, its utility is limited by the extreme steric constraints imposed by the C_6Me_6 ligand, which ultimately leads to the formation of dimeric products.

Acknowledgment is made to the donors of the Petroleum Research Fund, administered by the American Chemical Society, for the support of this research.

Supplementary Material Available: Listings of all bond lengths and angles, thermal parameters, and crystallographic data for $[(\eta^6\text{-C}_6\text{Me}_6)_2\text{Ru}_2(\mu\text{-NHPPh})_3][\text{BF}_4]$ (4 pages); a table of calculated and observed structure factors (15 pages). Ordering information is given on any current masthead page.

- (9) Gutowsky, H. S.; Holm, C. H. *J. Chem. Phys.* **1956**, *25*, 1228.
 (10) Jackman, L. M. In *Dynamic Nuclear Magnetic Resonance Spectroscopy*; Jackman, L. M., Cotton, F. A., Eds.; Academic Press: New York, 1975; pp 203-252.

Contribution from the Department of Chemistry and Ames Laboratory,¹ Iowa State University, Ames, Iowa 50011

The Layered, Metallic Scandium Iodide $\text{Sc}_{0.93}\text{I}_2$: Synthesis, Structure, and Properties

B. C. McCollum, D. S. Dudis, A. Lachgar, and J. D. Corbett*

Received September 6, 1989

The scandium halides form a wide variety of novel ternary phases, $\text{Sc}_5\text{Cl}_8\text{C}$,² $\text{Sc}_4\text{Cl}_6\text{B}$,³ $\text{Sc}_7\text{I}_2\text{C}$,⁴ $\text{Sc}_6\text{I}_{11}\text{C}_2$,⁵ and $\text{Sc}_7\text{I}_{12}\text{Co}$,⁶

for example, in which the third element listed is strongly bonded as an interstitial within each scandium cluster. However, scandium also forms several binary reduced halides that are evidently unique to this element. These include the very fibrous Sc_2Cl_3 and Sc_2Br_3 of unknown structure⁷ as well as the off-stoichiometry diiodide detailed here. The last was very briefly described years ago⁸ as a metallic phase with a CdI_2 -type structure and the composition $\text{ScI}_{2.17}$ for samples prepared by equilibration of liquid ScI_3 with excess metal. The composition and structure are unusual since all other metallic iodides appear to be fully reduced diiodides, viz. LaI_2 , CeI_2 , PrI_2 ,^{9,10} GdI_2 ,¹¹ and ThI_2 ,¹² and to occur principally in other structure types (TiSi_2 , MoS_2 , $\text{Mo}_4\text{S}_4\text{Br}_4$,¹³ NbS_2 ,¹⁴). Although the neighboring TiI_2 and Vl_2 exhibit CdI_2 -type structures, they are evidently of simple stoichiometry and are semiconductors.¹⁵

The original studies¹⁶ of this scandium iodide have remained largely unpublished because the structural investigations based on Debye-Scherrer powder diffraction patterns alone had difficulty in resolving the pattern of the reduced product from the very similar overlapping result for ScI_3 (BiI_3 -type). The patterns were further complicated by weak extra lines in the patterns of intermediate compositions; these probably arose from ternary phases formed by traces of impurities, carbon for example, that have been discovered since (above). We have now confirmed the stoichiometry and clarified the structure through studies of the synthesis via vapor-phase transport as well as by Guinier powder and single-crystal X-ray diffraction, and we report here the collection of results.

Experimental Section

All compounds were handled in gloveboxes under either dry N_2 or Ar. The scandium metal was an Ames Laboratory product prepared by reduction of ScF_3 with triply distilled Ca. The material used in the later studies had also been vacuum-sublimed, and its typical impurity levels have been described.³ The earlier investigations of the phase diagram and other properties utilized metal that had higher impurities in some cases (ppm by weight): 0, 300; F, 250; Ta, 1500-2000; Y, 100. Turnings were used in the ScI_3 synthesis and phase studies, while chunks or rolled strips were used in equilibrations. The triiodide was again⁴ prepared from the elements in a two-zone silica apparatus with the metal held in a W crucible in the hotter zone. The product was then sublimed three times under high vacuum ($\sim 10^{-5}$ atm) at ~ 680 °C within a tantalum apparatus contained in a silica jacket. The pure product is bright yellow, not white.¹⁷ We found that the melting point of the product decreased $\sim 10^\circ$ when the triiodide was sublimed so that it condensed on the SiO_2 jacket rather than in a Ta sleeve, doubtlessly because the former introduces ScOI through a metathetical reaction between ScI_3 and SiO_2 .

The so-called diiodide is readily obtained by reaction of liquid or gaseous ScI_3 with excess metal in the range 550-870 °C for about 6 weeks to 4 days, respectively, while contained in welded Ta or Nb containers. The powder patterns obtained with an Enraf-Nonius FR552 Guinier camera show no evidence of ScI_3 in the products, and the analyses (below) by both wet and X-ray methods support the formation of a pure phase.

Thermal analyses of the ScI_3 -Sc system out to 35.1 mol % Sc gave

- (1) Ames Laboratory—DOE is operated for the U.S. Department of Energy by Iowa State University under Contract No. W-7405-Eng-82.
 (2) Hwu, S.-J.; Dudis, D. S.; Corbett, J. D. *Inorg. Chem.* **1987**, *26*, 469.
 (3) Hwu, S.-J.; Corbett, J. D. *J. Solid State Chem.* **1986**, *64*, 331.
 (4) Dudis, D. S.; Corbett, J. D.; Hwu, S.-J. *Inorg. Chem.* **1986**, *25*, 3434.
 (5) Dudis, D. S.; Corbett, J. D. *Inorg. Chem.* **1987**, *26*, 1933.
 (6) Hughbanks, T.; Corbett, J. D. *Inorg. Chem.* **1988**, *27*, 2022.
 (7) McCollum, B. C.; Camp, M. J.; Corbett, J. D. *Inorg. Chem.* **1973**, *12*, 778.
 (8) McCollum, B. C.; Corbett, J. D. *Chem. Commun.* **1968**, 1666.
 (9) Corbett, J. D.; Druding, L. F.; Burkhard, W. J.; Lindahl, C. B. *Discuss. Faraday Soc.* **1961**, *32*, 79.
 (10) Corbett, J. D.; Sallach, R. A.; Lokken, D. L. *Adv. Chem. Ser.* **1967**, *No. 71*, 56.
 (11) Mee, J. E.; Corbett, J. D. *Inorg. Chem.* **1965**, *4*, 88.
 (12) Clark, R. J.; Corbett, J. D. *Inorg. Chem.* **1963**, *2*, 460.
 (13) (a) Warkentin, E.; Bärnighausen, H. Z. *Anorg. Allg. Chem.* **1979**, *459*, 187. (b) Warkentin, E.; Bärnighausen, H. Unpublished research.
 (14) Guggenberger, L. J.; Jacobson, R. A. *Inorg. Chem.* **1968**, *7*, 2257.
 (15) Wilson, J. A. *Adv. Phys.* **1972**, *21*, 145.
 (16) McCollum, B. C. Ph.D. Dissertation, Iowa State University, 1970.
 (17) Brown, D. *Halides of the Lanthanides and Actinides*; J. Wiley: London, 1968; p 218.